Biochemical and Biophysical Research Communications 452 (2014) 1067–1070

Contents lists available at ScienceDirect

Biochemical and Biophysical Research Communications

journal homepage: www.elsevier.com/locate/ybbrc

K-rasG12V mediated lung tumor models identified three new quantitative trait loci modifying events post-*K-ras* mutation

Hiromitsu Saito, Noboru Suzuki *

Department of Animal Genomics, Functional Genomics Institute, Mie University Life Science Research Center, 2-174 Edobashi, Tsu, Mie 514-8507, Japan

ARTICLE INFO

Article history:
Received 10 September 2014
Available online 20 September 2014

Keywords:
Genetic susceptibility
K-ras oncogenes
Lung cancer
Modifier gene
QTL

ABSTRACT

A high incidence of oncogenic *K-ras* mutations is observed in lung adenocarcinoma of human cases and carcinogen-induced animal models. The process of oncogenic *K-ras*-mediated lung adenocarcinogenesis can be dissected into two parts: pre- and post-*K-ras* mutation. Adoption of transgenic lines containing a *flox-K-rasG12V* transgene eliminates the use of chemical carcinogens and enables us to study directly crucial events post-*K-ras* mutation without considering the cellular events involved with oncogenic *K-ras* mutation, e.g., distribution and metabolism of chemical carcinogens, DNA repair, and somatic recombination by host factors. We generated two mouse strains C57BL/6J-*Ryr2*^{tm1Nobs} and A/J-*Ryr2*^{tm1Nobs} in which *K-rasG12V* can be transcribed from the cytomegalovirus early enhancer/chicken beta actin promoter in virtually any tissue. Upon *K-rasG12V* induction in lung epithelial cells by an adenovirus expressing the Cre recombinase, the number of tumors in the C57BL/6J-*Ryr2*$^{tm1Nobs/+}$ mouse line was 12.5 times that in the A/J-*Ryr2*$^{tm1Nobs/+}$ mouse line. Quantitative trait locus (QTL) analysis revealed that new three modifier loci, *D3Mit19*, *D3Mit45* and *D11Mit20*, were involved in the differential susceptibility between the two lines. In addition, we found that differential expression of the wild-type *K-ras* gene, which was genetically turn out to be anti-oncogenic activity on *K-rasG12V*, could not account for the different susceptibility in our two *K-rasG12V*-mediated lung tumor models. Thus, we provide a genetic system that enables us to explore new downstream modifiers post-*K-ras* mutation.

1. Introduction

Wild-type K-ras is a membrane-associated GTP signaling protein that regulates cell proliferation, differentiation, and survival [1]. Missense mutations at codons 12, 13, or 61 result in decreased GTPase activity and constitutive signaling, which are potently oncogenic. Indeed, about 30% of all human lung adenocarcinomas feature mutated *K-ras*. The mutation appears to be involved in an early stage of lung adenocarcinogenesis [2]. In animal models, two groups demonstrated that sporadic expression of the oncogenic *K-ras* gene was sufficient to elicit lung tumorigenesis [3,4]. Thus, exploring the genetic factors involved in tumor growth and multiplicity post-*K-ras* mutation is important for preventing lung tumor progression. QTL analysis using chemical carcinogen-induced mouse lung tumor models has identified many tumor modifier loci, variously termed *pulmonary adenoma susceptibility* (*Pas*), *pulmonary adenoma resistance* (*Par*), and *susceptibility to lung cancer* (*Sluc*) [5]. The involvement of these loci in pre- and post-*K-ras* mutational events remains unclear, because chemical carcinogens can be involved in both events. However, oncogenic *K-ras* tumorigenesis using the *Cre*/*loxP* system allows us to focus on post-*K-ras* mutational events. Here, we report two *K-rasG12V*-driven mouse strains, namely, C57BL/6J-*Ryr2*^{tm1Nobs} and A/J-*Ryr2*^{tm1Nobs}, which have high- and low-lung tumorigenicity, respectively, upon lung-specific *K-rasG12V* overexpression.

2. Materials and methods

2.1. Animals

C57BL/6J-*Ryr2*$^{tm1Nobs/+}$ and A/J-*Ryr2*$^{tm1Nobs/+}$ mice were established by breeding the original *Ryr2*^{tm1Nobs} strain [6] with C57BL/6J Jms Slc and A/J Jms Slc mice, respectively, through 12 generations. Intercross C57BL6/JA/JF2-*Ryr2*$^{tm1Nobs/+}$ mice were generated by first breeding male A/J-*Ryr2*$^{tm1Nobs/+}$ mice with female C57BL/6J-*Ryr2*$^{tm1Nobs/+}$ mice, and then using the wild-type female A/JC57BL6/JF1 animals to breed with male A/JC57BL6/JF1-*Ryr2*$^{tm1Nobs/tm1Nobs}$ mice. The Animal care and Use committee of Mie University approved the protocol (Permit number: 24–23). All surgery was performed under sodium pentobarbital or isoflurane anesthesia, and all efforts were made to minimize suffering.

* Corresponding author. Fax: +81 59 231 5220.
E-mail address: nsuzuki@doc.medic.mie-u.ac.jp (N. Suzuki).

http://dx.doi.org/10.1016/j.bbrc.2014.09.052
0006-291X/

2.2. Ad-Cre infection-induced tumors

The lungs of 8-week-old male A/J-*Ryr2*$^{tm1Nobs/+}$ and C57BL/6J-*Ryr2*$^{tm1Nobs/+}$ mice were infected with Ad-Cre (Cosmo Bio Company, Japan) by intratracheal administration. Briefly, the mice were anesthetized with pentobarbital sodium salt (50 mg/kg body weight). The trachea was reached via a craniocaudal incision in the neck. A 5-μL aliquot containing 2×10^9 plaque-forming units (pfu)/mL was injected. The mice were sacrificed 8 weeks after infection, and the lungs were fixed with 4% PFA/PBS and stained with LacZ, as previously described [7], for microscopic and histological analyses.

2.3. Count of tumor numbers

The numbers of LacZ positive lesions of whole mount stained lungs were counted under stereoscopic microscope (Leica, Germany).

2.4. Histological analysis

Histological analysis was performed as described [7]. The antibodies used were rabbit anti-human surfactant apoprotein-C (SP-C) (1:200; RDI, USA), goat anti-Clara cell antigen (CC10) (1:200; Santa Cruz Biotechnology, USA), HRP-conjugated donkey anti-goat immunoglobulin G (IgG) (1:1000; Santa Cruz Biotechnology), and HRP-conjugated goat anti-rabbit IgG (1:200; Chemicon International, USA).

2.5. Statistical analysis

The paired Student's *t*-test was used for statistical analysis of the significance of differences between the two. A *P* value of <0.05 was considered statistically significant.

2.6. Genotyping

Genomic DNA was extracted as described [7]. We genotyped intercross F2 mice ($n = 96$) using sequencing length polymorphism markers, *Kras2–37*, *D3Mit19*, *D3Mit45*, *D3Mit319*, *D3Mit11*, *D3Mit60*, *D11Mit336*, *D11Mit4*, *D11Mit164*, *D11Mit20*, *D11Mit229*, and *D11Mit79* [8,9] by PCR. The PCR conditions were 95 °C for 2 min; 40 cycles of 98 °C for 10 s, 55 °C for 30 s and 68 °C for 1 min; and 68 °C for 5 min.

3. Results and discussion

We bred the *Ryr2*^{tm1Nobs} allele [6] into the C57BL/6J and A/J strains to establish the C57BL/6J-*Ryr2*^{tm1Nobs} and the A/J-*Ryr2*^{tm1Nobs} strains, respectively. At 8 weeks after intratracheal administration of Ad-Cre, we detected *K-rasG12V*-expressing tumors (Fig. 1A and B). The tumor incidence of the C57BL/6J-*Ryr2*$^{tm1Nobs/+}$ and A/J-*Ryr2*$^{tm1Nobs/+}$ mice were 100% (6/6) and 80% (4/5), respectively. The C57BL/6J-*Ryr2*$^{tm1Nobs/+}$ mice (142 ± 59.5 tumors/mouse) demonstrated a 12-fold higher susceptibility than A/J-*Ryr2*$^{tm1Nobs/+}$ mice (11.4 ± 14.8 tumors/mouse; mean ± SD, $P = 0.001$) (Fig. 1C). In addition, the mean tumor size in the C57BL/6J-*Ryr2*$^{tm1Nobs/+}$mice (319 ± 87 μm) was significantly larger than that in the A/J-*Ryr2*$^{tm1Nobs/+}$ mice (268 ± 93 μm; mean ± SD, $P = 0.006$). The insertion of the *flox-K-rasG12V* transgene had no detectable influence both on gene expression and function of *Ryr2* (data not shown) and on the original chemical carcinogen (urethane)-induced lung tumor sensitivity (Fig. S1) in the lungs of these mice. After infection, the two strains showed no difference in *K-rasG12V* expression, uniform Cre protein expression and the infection kinetics of the lung cells (Fig. S2A–D). These results suggest that the differential susceptibility of the two lines was not due to differential transgene expression level and efficiency of virus infection.

Histological analysis at 8 weeks after induction demonstrated that the lung lesions in both C57BL/6J-*Ryr2*$^{tm1Nobs/+}$ and A/J-*Ryr2*$^{tm1Nobs/+}$ mice were typical adenomas featured with papillary architecture (Fig. 2A and B). The adenomas from both lines stained strongly and uniformly for SP-C for alveolar type II cells, indicating that these arose from alveolar type II cells or their precursors (Fig. 2C and D). Furthermore, CC10 staining of the central portions of the tumors suggested that SP-C and CC10 double-positive putative bronchi alveolar stem cells were contained in the C57BL/6J-*Ryr2*$^{tm1Nobs/+}$ mouse tumors at this stage (Fig. 2E and F).

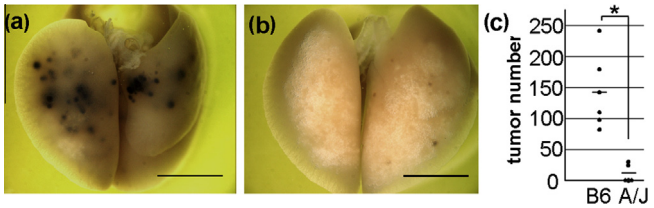

Fig. 1. Lung tumor susceptibilities to *K-rasG12V* induction in C57BL/6J-*Ryr2*$^{tm1Nobs/+}$ and A/J-*Ryr2*$^{tm1Nobs/+}$ mice. (A and B) Whole-mount views of LacZ-stained lungs of C57BL/6J-*Ryr2*$^{tm1Nobs/+}$ (A) and A/J-*Ryr2*$^{tm1Nobs/+}$ (B) mice. LacZ-staining verified *K-rasG12V* expression in the tumors. (C) Lung tumor multiplicities of C57BL/6J-*Ryr2*$^{tm1Nobs/+}$ ($n = 6$) and A/J-*Ryr2*$^{tm1Nobs/+}$ mice ($n = 5$). The mean multiplicities for each genotype is indicated by a line. $^*P < 0.05$. Abbreviations: B6, C57BL/6J-*Ryr2*$^{tm1Nobs/+}$ mice; A/J, A/J-*Ryr2*$^{tm1Nobs/+}$ mice. Scale bar: 5.0 mm for A and B.

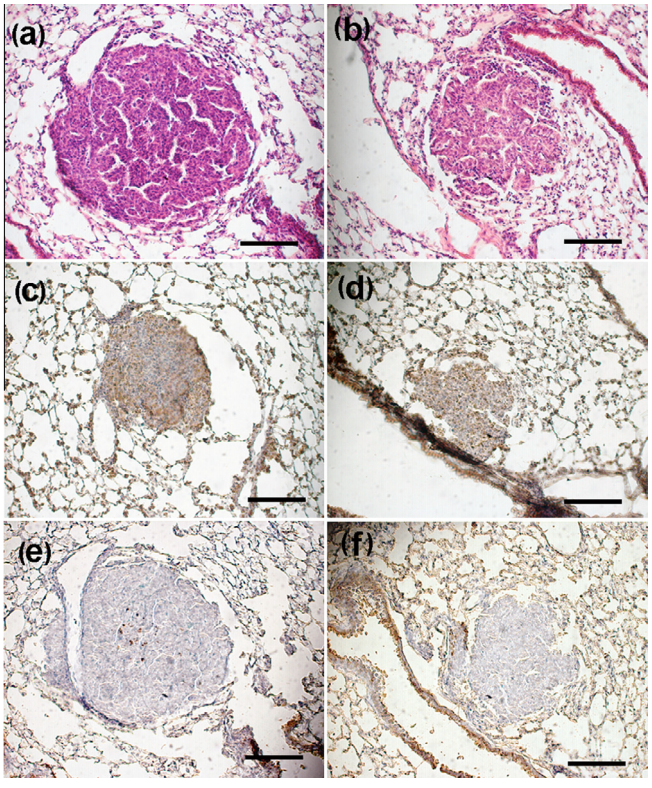

Fig. 2. Histology of *K-rasG12V*-driven lung tumors of C57BL/6J-*Ryr2*$^{tm1Nobs/+}$ and A/J-*Ryr2*$^{tm1Nobs/+}$ mice. (A and B) Hematoxylin and eosin-stained section of C57BL/6J-*Ryr2*$^{tm1Nobs/+}$ (A) and A/J-*Ryr2*$^{tm1Nobs/+}$ (B) mice lung tumors. (C–F) Immunostaining of lung tumors of C57BL/6J-*Ryr2*$^{tm1Nobs/+}$ (C and E) and A/J-*Ryr2*$^{tm1Nobs/+}$ (D and F) mice with anti-SP-C (C and D), anti-CC10 (E and F) antibodies (brown) counterstained with hematoxylin (C–F). Tumors were sampled at 8 weeks after *K-rasG12V* induction. Scale bar: 100 μm for A–F. (For interpretation of the references to colour in this figure legend, the reader is referred to the web version of this article.)

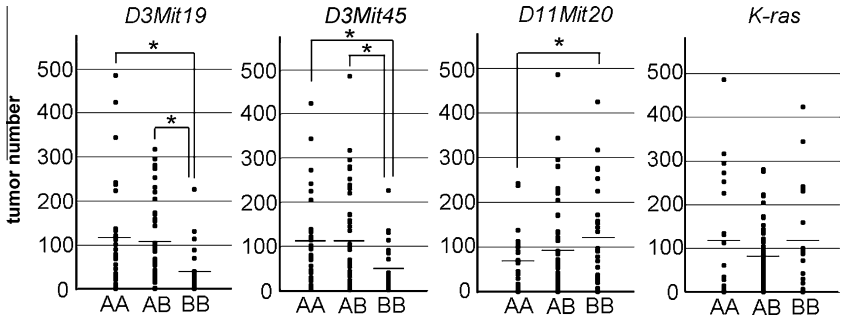

Fig. 3. Lung tumor multiplicities. Total number of surface lung tumors was determined under a dissecting microscope. Abbreviations: AA, the A/J allele homozygote mice; BB, the C57BL/6 allele homozygote mice; AB, A/J and C57BL/6 allele heterozygote mice. The mean multiplicities for each genotype is indicated by a line. *$P < 0.05$.

Table 1
Average lung tumor number and correlation with genotype.

Markers (cM)	Genotype			*P* value
	AA	AB	BB	(AA vs BB)
D3Mit19 (87.6)	115.3 ($n = 30$)	107.1 ($n = 48$)	44.9 ($n = 18$)	0.030*
D3Mit45 (72.43)	110.2 ($n = 27$)	110.3 ($n = 48$)	54.4 ($n = 21$)	0.040*
D3Mit319 (56.84)	92.7 ($n = 23$)	107.4 ($n = 50$)	82.9 ($n = 23$)	0.705
D3Mit11 (43.71)	99.8 ($n = 18$)	96.0 ($n = 54$)	101.3 ($n = 24$)	0.965
D3Mit60 (1.96)	94.7 ($n = 17$)	95.7 ($n = 56$)	122.9 ($n = 23$)	0.729
D11Mit336 (73.75)	94.1 ($n = 26$)	94.1 ($n = 46$)	109.7 ($n = 24$)	0.549
D11Mit4 (41.87)	87.8 ($n = 23$)	89.1 ($n = 47$)	123.3 ($n = 26$)	0.215
D11Mit164 (34.5)	74.4 ($n = 23$)	97.8 ($n = 52$)	124.6 ($n = 21$)	0.095
D11Mit20 (27.23)	67.5 ($n = 21$)	96.2 ($n = 50$)	127.2 ($n = 25$)	0.042*
D11Mit229 (15.63)	69.0 ($n = 23$)	119.7 ($n = 45$)	87.1 ($n = 28$)	0.427
D11Mit79 (12.35)	83.3 ($n = 24$)	125.8 ($n = 47$)	60.0 ($n = 25$)	0.294
K-ras	120.8 ($n = 21$)	80.3 ($n = 55$)	122.9 ($n = 20$)	0.960

* $P < 0.05$.

Two groups [10,11] suggested previously that the expression balance of wild-type and mutant *K-ras* might determine the genetic susceptibility to mouse lung tumorigenesis. The expression levels of wild-type *K-ras* in the C57BL/6J-*Ryr2*$^{tm1Nobs/+}$ mouse lungs were 0.73 times higher (±SD, ±0.087; $P = 0.01$) than that in the A/J-*Ryr2*$^{tm1Nobs/+}$ mouse lungs (mean ± SD, 1.00 ± 0.057) (Fig. S2E). To evaluate the relationship between the *K-ras* gene locus and the tumor multiplicity driven by induced *K-rasG12V* in our mice, we analyzed QTLs of 96 F2 intercross mice using the *K-ras* gene polymorphisms in the second intron sequences [8,12] and no significant linkage was found (Fig. 3 and Table 1). Thus, our two strains might enable us to search for specific modifier genes other than wild-type *K-ras*.

Next, to evaluate the efficacy of our strains exploring new modifier genes, we obtained panels of F2 intercross mice for genotyping with panels of microsatellites at ~20 cM density on chromosome 3 and 11. Because these have no and three chemically induced-lung tumor susceptible QTLs, respectively [5]. By single point analysis, we identified significant two loci, *D3Mit19* and *D3Mit45*, on chromosome 3 and one, *D11Mit20*, on chromosome11, which increase and decrease *K-rasG12V*-induced lung tumor multiplicity of F2 mice with A/J strain derived loci, respectively (Fig. 3 and Table 1). Interestingly, *D3Mit19* was mapped to the QTL controlling both pulmonary PKC activity and PKC-α content which were higher in B6 than in A/J lung [13]. High PKC-α levels are associated with a differentiated and proliferatively quiescent phenotype in mouse lung epithelium [14]. *D11Mit20* (27.23 cM) is located near *Jnk2* (29.96 cM) [15]. Oncogenic *K-ras*-driven lung tumors show activation of The JNK/SAP pathway [16] and their growth is impaired by the ablation of both *Jnk1* and *Jnk2* [17]. Taken together, *Jnk2* might be a candidate gene as oncogenic *K-ras*-downstream modifier on *D11Mit20* and more activated in C57BL/6J-*Ryr2*$^{tm1Nobs/+}$ genome than in A/J-*Ryr2*$^{tm1Nobs/+}$ genome.

These identified three loci were not associated with previously reported lung tumor susceptibility loci from QTL analyses using chemical carcinogen induced mouse models [5], suggesting that our two strains were useful tool to identify new lung tumor susceptible genes specifically involved in post-*K-ras* mutation. Investigating a genome-wide QTL analysis and exploring novel modifier genes are our next issues.

Disclosure statement

The authors have no conflict of interest.

Acknowledgments

This work was supported by internal funding from the Mie University.

Appendix A. Supplementary data

Supplementary data associated with this article can be found, in the online version, at http://dx.doi.org/10.1016/j.bbrc.2014.09.052.

References

[1] S.L. Campbell, R. Khosravi-Far, K.L. Rossman, et al., Increasing complexity of Ras signaling, Oncogene 17 (1998) 1395–1413.
[2] H. Kitamura, Y. Kameda, T. Ito, et al., Atypical adenomatous hyperplasia of the lung, Am. J. Clin. Pathol. 111 (1999) 610–622.

[3] E.L. Jackson, N. Willis, K. Mercer, et al., Analysis of lung tumor initiation and progression using conditional expression of oncogenic K-ras, Genes Dev. 15 (2001) 3243–3248.
[4] R. Meuwissen, S.C. Linn, M. van der Valk, et al., Mouse model for lung tumorigenesis through Cre/lox controlled sporadic activation of the K-Ras oncogene, Oncogene 20 (2001) 6551–6558.
[5] A.K. Bauer, A.M. Malkinson, S.R. Kleeberger, Susceptibility to neoplastic and non-neoplastic pulmonary diseases in mice: genetic similarities, Am. J. Physiol. Lung Cell Mol. Physiol. 287 (2004) L685–L703.
[6] H. Tsumura, T. Yoshida, H. Saito, et al., Cooperation of oncogenic *K-ras* and *p53* deficiency in pleomorphic rhabdomyosarcoma development in adult mice, Oncogene 25 (2006) 7673–7679.
[7] H. Saito, H. Tsumura, S. Otake, et al., *L7/Pcp-2*-specific expression of Cre recombinase using knock-in approach, Biochem. Biophys. Res. Commun. 331 (2005) 1216–1221.
[8] G. Manenti, A. Stafford, L.D. Gregorio, et al., Linkage disequilibrium and physical mapping of *Pas1* in mice, Genome Res. 9 (1999) 639–646.
[9] T. Sakai, S. Yamad-Ishibashi, Y. Wakita, et al., Update of mouse microsatellite database of Japan (MMDBJ), Exp. Anim. 53 (2004) 151–154.
[10] Z. Zhang, Y. Wang, H.G. Vikis, et al., Wildtype Kras2 can inhibit lung carcinogenesis in mice, Nat. Genet. 29 (2001) 25–33.
[11] D.M. To, J. Perez-Losada, J. Mao, et al., A functional switch from lung cancer resistance to susceptibility at *Pas1* locus in $Kras^{LA2}$ mice, Nat. Genet. 38 (2006) 926–930.
[12] B. Chen, L. Johanson, J.S. Wiest, et al., The second intron of the *K-ras* gene contains regulatory elements associated with mouse lung tumor susceptibility, Proc. Natl. Acad. Sci. U.S.A. 91 (1994) 1589–1593.
[13] L.D. Dwyer-Nield, B. Paigen, S.E. Porter, et al., Quantitative trait locus mapping of genes regulating pulmonary PKC activity and PKC-α content, Am. J. Physiol. Lung Cell Mol. Physiol. 279 (2000) L326–L332.
[14] L.D. Dwyer, A.C. Miller, A.L. Parks, et al., Calpain-induced downregulation of activated protein kinase C-alpha affects lung epithelial cell morphology, Am. J. Physiol. 266 (1994) L569–L576.
[15] A. Cox, C.L. Ackert-Bicknell, B.L. Dumout, et al., A new standard genetic map for the laboratory mouse, Genetics 182 (2009) 1335–1344.
[16] Y. Zhou, W.M. Rideout 3rd, T. Zi, et al., Chimeric mouse tumor models reveal differences in pathway activation between ERBB family- and KRAS-dependent lung adenocarcinomas, Nat. Genet. 28 (2010) 71–78.
[17] C. Cellurale, G. Sabio, N.J. Kennedy, et al., Requirement of c-Jun NH2-terminal kinase for Ras-initiated tumor formation, Mol. Cell. Biol. 31 (2011) 1565–1576.